Received: 4 December 2024 | Accepted: 23 June 2025

DOI: 10.1111/2041-210X.70110

Methods in Ecology and Evolution

RESEARCH ARTICLE

Renewal equations for mosquito-borne diseases

Cathal Mills[1,2] | Tarek Alrefae[1,2] | William S. Hart[3] | Moritz U. G. Kraemer[2,4] | Kris V. Parag[5] | Robin N. Thompson[3] | Christl A. Donnelly[1,2] | Ben Lambert[1]

[1]Department of Statistics, University of Oxford, Oxford, UK

[2]Pandemic Sciences Institute, University of Oxford, Oxford, UK

[3]Mathematical Institute, University of Oxford, Oxford, UK

[4]Department of Biology, University of Oxford, Oxford, UK

[5]MRC Centre for Global Infectious Disease Analysis, Imperial College London, London, UK

Correspondence
Cathal Mills
Email: cathal.mills@linacre.ox.ac.uk

Funding information
Google.org; Oxford Martin School, University of Oxford; Medical Research Foundation, Grant/Award Number: MRF-RG-ICCH-2022-100069; Engineering and Physical Sciences Research Council, Grant/Award Number: APP8583 and EP/T517811/1; National Institute for Health Research Health Protection Research Unit, Grant/Award Number: HPRU200907; John Fell Fund, University of Oxford; Rockefeller Foundation, Grant/Award Number: PC-2022-POP-005; European Union Horizon Europe programme project E4Warning, Grant/Award Number: 101086640; European Union's Horizon Europe programme project MOOD, Grant/Award Number: 874850; Branco Weiss Fellowship - Society in Science, Grant/Award Number: 225288/Z/22/Z, 226052/Z/22/Z, 228186/Z/23/Z and 303666/Z/23/Z; Kuwait Foundation for the Advancement of Sciences; Medical Research Council, Grant/Award Number: MR/X020258/1; Department for International Development, UK Government, Grant/Award Number: 301542-403; Bill & Melinda Gates Foundation, Grant/Award Number: INV-063472; Novo Nordisk Foundation, Grant/Award Number: NNF24OC0094346

Handling Editor: Matthew Silk

Abstract

1. During infectious disease outbreaks, estimates of time-varying pathogen transmissibility, such as the instantaneous reproduction number $R(t)$ or epidemic growth rate r_t, are used to inform decision-making by public health authorities. For directly transmitted infectious diseases, the renewal equation framework is a widely used method for measuring time-varying transmissibility. The framework uses information on the typical time elapsing between an infection and the offspring infections (quantified by the generation time distribution), and $R(t)$, to describe the rate at which currently infected individuals generate new infections, if conditions affecting human transmission were to remain the same as at time t.
2. For diseases with transmission cycles involving hosts and vectors, however, renewal equation models have been far less used. This is likely due to difficulties in mechanistically defining generation times that can capture the complexity of multi-stage, human-vector relationships.
3. Here, using dengue as an example, we provide general renewal equations that are derived from first principles using age-structured systems of coupled partial differential equations across human and vector sub-populations. Our framework tracks the multi-stage transmission cycle over calendar time and across stage-specific ages, resulting in governing renewal equations that quantify how the rate at which new infections are generated from existing infections depends on stage-specific processes. In a numerical application to real-world temperature data, we show how the generation time distribution depends on both current and historical conditions.
4. The framework provides a foundation on which to base inferential frameworks for estimating $R(t)$ and r_t for infectious diseases with multiple stages in the transmission cycle.

KEYWORDS
climate change, dengue, generation time, infectious disease modelling, mosquito, renewal equations, reproduction number, vector-borne diseases

1 | INTRODUCTION

In infectious disease epidemiology, renewal equations can be used to describe how new infections are generated from individuals infected in the past. The time period that elapses between a previous infection and a new infection caused by it is called the generation time, and the variation in this time period across individuals is captured by the generation time distribution (Svensson, 2007). The number of infections, on average, that a given infected human would generate (should conditions affecting human transmission remain the same) throughout the course of their infection is known as the instantaneous reproduction number, $R(t)$ (Fraser, 2007).

For directly transmitted (human-to-human) infectious diseases, renewal equation frameworks have found widespread use for estimating $R(t)$. The popularity is likely in part due to the relatively few assumptions needed to produce $R(t)$ estimates compared to other frameworks such as compartmental models. By fitting renewal equation models to time series of infection counts, or more commonly, case counts, it is possible to estimate $R(t)$, and these models form the basis for many popular approaches and software used to infer changes in transmission throughout outbreaks (Abbott et al., 2020; Cori et al., 2013; Fraser, 2007; Parag, 2021; Thompson et al., 2019). A renewal equation model for a directly transmitted infectious disease may be described by

$$i(t) = R(t) \int_0^\infty i(t-\tau) w(\tau) d\tau, \tag{1.1}$$

where $i(t)$ is the number of new infections generated at time t, $R(t)$ is the instantaneous reproduction number at time t, and $w(\tau)$ is the probability density that describes the generation time distribution, resulting in $\int_0^\infty w(\tau) = 1$. Equation (1.1) intuitively gives a process by which previous infections beget new infections with some time delay, and if $R(t) > 1$, the epidemic would grow in the long term if conditions affecting human transmission were to remain the same as at time t. Consequently, the threshold of $R(t) > 1$ coincides with an instantaneous epidemic growth rate $r_t > 0$, where r_t is the rate of change of the log infection incidence in calendar time.

The renewal equation is most often implemented in discrete time to align with the temporal resolution of surveillance data (Ogi-Gittins et al., 2023). Renewal models, as used for inference, also often include stochasticity (e.g. Pakkanen et al., 2023). Misspecification of the generation time distribution can be a large potential source of error in this estimation of $R(t)$ (Parag et al., 2022, 2023; Park et al., 2022, 2024), and given the popularity of $R(t)$ for informing public health policy and decision-making (Vegvari et al., 2022), the violation of the assumption of time-invariant generation times clearly has practical, real-world consequences.

For infectious diseases with a single population (equivalently, a single transmission stage) and a static generation time distribution, continuous renewal equations (such as Equation 1.1) can be derived from a partial differential equation (PDE) representation of the infection-age-structured model of the infected population; this was first derived by Kermack and McKendrick (Champredon et al., 2018; Kermack & McKendrick, 1927; Keyfitz & Keyfitz, 1997). The renewal equation can also be used to estimate so-called state reproduction numbers, starting from an age-structured system with multiple host populations (Inaba & Nishiura, 2008). We provide a short description of these methods in Appendix A, and for a more complete primer on renewal equations for directly transmitted diseases (see Bouros et al., 2025).

For vector-borne diseases, renewal equations are less commonly used as (i) it is unclear whether the popular renewal equation can generalise to the multi-stage transmission cycle across various host and vector sub-populations (e.g. four stages for dengue across mosquito and human populations, Figure 1) and (ii) the common assumption in renewal equations (as in Equation 1.1) of a static generation time distribution is often unrealistic for climate-sensitive, vector-borne diseases. Under laboratory conditions, several mosquito-viral traits, such as the extrinsic incubation period, the rate of mosquito blood feeding and mosquito density, have been shown to be influenced by climate factors such as temperature (Chan & Johansson, 2012; Mordecai et al., 2017, 2019). Also, the time taken for an infectious (or susceptible) mosquito to bite a susceptible (infectious) human will depend on susceptible human (mosquito) population levels.

Existing approaches have used temperature data to parameterise temperature-dependent, time-varying generation times to estimate basic (R_0) and instantaneous reproduction numbers ($R(t)$). These approaches often involve a convolution of probability densities for the stages of the dengue transmission cycle, Ross-Macdonald assumptions for mosquito-borne pathogens and/or parametric distributions for temperature-dependent generation times (Codeço et al., 2018; Mordecai et al., 2019; Romeo-Aznar et al., 2024; Ross, 1910; Siraj et al., 2017; Smith et al., 2012). For example, one such existing approach is (Siraj et al., 2017) which provided formulae for a time-varying generation time distribution based on current temperatures. Such approaches, however, do not provide a mechanistically derived generation time distribution—as the relative contributions of previously infected humans and mosquitoes to new human infections. Another approach for vector-borne diseases has used renewal equations, albeit with a static generation time distribution (Perkins et al., 2015).

Here, we adopt a different approach by deriving renewal equations for a vector-borne disease starting from an age-structured system of coupled PDEs. To the best of our knowledge, this is the first derivation of renewal equations from first principles for a vector-borne disease. In doing so, we derive a mechanistically based generation time distribution which informs estimates of

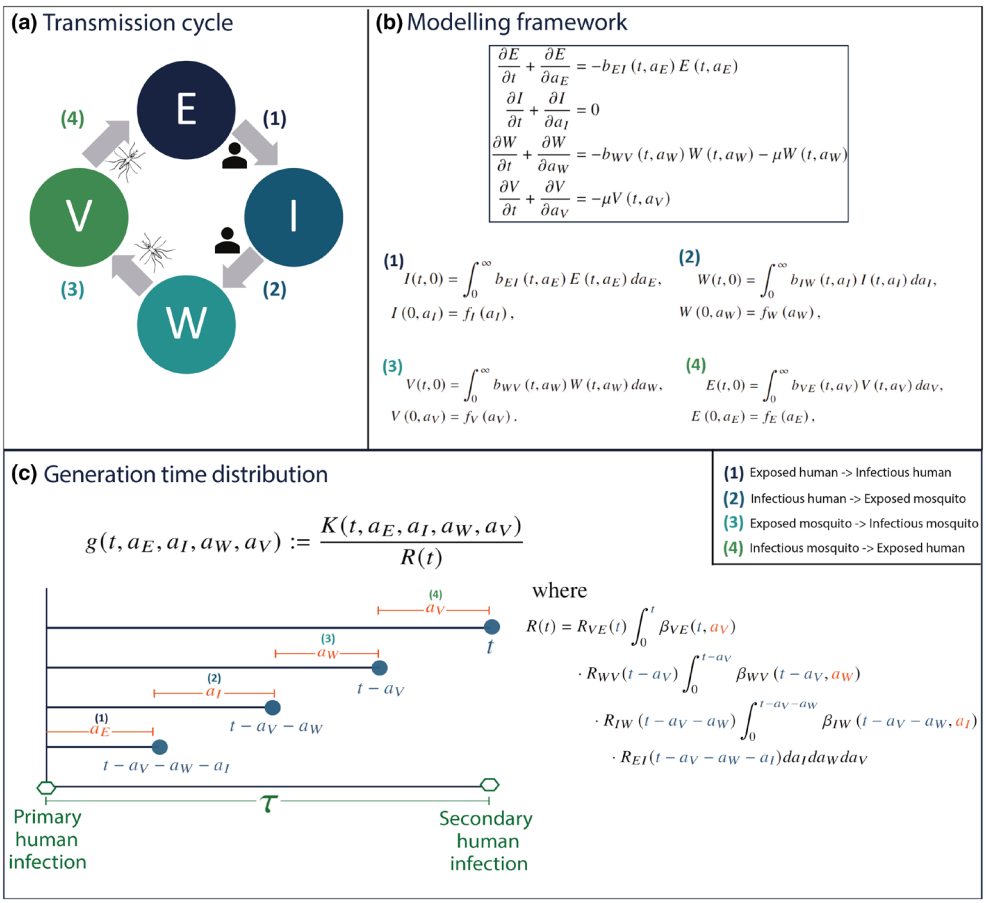

FIGURE 1 Schematic of key concepts used to estimate $R(t)$ for mosquito-borne diseases. (a) The four-stage transmission cycle for dengue—from exposed humans (E) to infectious humans (I) to exposed mosquitoes (W) to infectious mosquitoes (V). The boundary conditions (numbered) of our modelling framework generate entries into each sub-population. (b) Our full modelling framework, Equations (2.21–2.32), including the PDEs and their boundary and initial conditions. (c) The generation time distribution at calendar time t, described by $g(t,a_E,a_I,a_W,a_V)$, is obtained by normalising the instantaneous kernel $K(t,a_E,a_I,a_W,a_V)$ using $R(t)$. $R(t)$ can be estimated using between-stage reproduction numbers and generation times using ages (orange) at intermediate calendar times (blue) when generation events (i.e. stage transitions) occur.

$R(t)$ from our renewal equation, where $R(t)$ retains the same interpretation (as for directly transmitted diseases)—the number of infections, on average, that a given infected human would generate (should conditions affecting human transmission at time t remain the same) throughout the course of their infection. Throughout, we use dengue as a case-study to motivate and develop our renewal equations, yet our approach can generalise to other mosquito-borne diseases (e.g. Zika, malaria or yellow fever).

2 | METHODS AND RESULTS

2.1 | Infection-age-structured human and mosquito populations

2.1.1 | Modelling framework

To illustrate the calculation steps for our full model of the dengue transmission cycle (Section 2.2), we start with a simplified abstraction of the dengue transmission cycle. We do not explicitly track the calendar times when a human (mosquito) becomes infectious after the viral infection event (i.e. after a mosquito bites a human). Our age-structured framework (further details of our framework are in Appendix B) describes both the infected mosquito and human populations using continuity equations: the McKendrick–von Foerster equation (McKendrick, 1925; Murray, 2002).

Our system of age-structured populations is described by the following conservation equations:

$$\frac{\partial E}{\partial t}+\frac{\partial E}{\partial a_E}=0, \tag{2.1}$$

$$\frac{\partial M}{\partial t}+\frac{\partial M}{\partial a_M}=-\mu M(t,a_M), \tag{2.2}$$

where t denotes calendar time, $E\geq 0$ and $M\geq 0$ denote the density of the infected human and mosquito populations respectively with corresponding ages $a_E\geq 0$ and $a_M\geq 0$, and $\mu>0$ is the (fixed) mortality rate in the infectious mosquito population. The variables a_E and a_M

denote the time since entering the stage (not the age of a mosquito/human). For example, $E(t=3, a_E=2)$ denotes the density of humans who were infected two time units (e.g. days) before calendar time $t=3$. Each first-order linear equation, Equations (2.1–2.2), posits that, because age a_C (defined as time since entry to a sub-population C) and calendar time t are measured in the same units, the rate at which a sub-population ages would equal the rate of population change with respect to time in the absence of any instantaneous death rate (i.e. the rate at which individuals leave a sub-population C). See Murray (Murray, 2002) Chapter 1.7 for more details.

We close the system with the following boundary conditions:

$$E(t,0)=\int_0^{\infty} b_{ME}(t,a_M)M(t,a_M)da_M, \tag{2.3}$$

$$E(0,a_E)=f_E(a_E), \tag{2.4}$$

$$M(t,0)=\int_0^{\infty} b_{EM}(t,a_E)E(t,a_E)da_E, \tag{2.5}$$

$$M(0,a_M)=f_M(a_M), \tag{2.6}$$

where $f_E(a_E)$ and $f_M(a_M)$ denote the initial densities of infected human and mosquito populations, and each $b_{CD}(t,a_C)\geq 0$ is a time- and age-dependent birth function that represents the rate at which new individuals in sub-population D are generated at calendar time t by an individual of age a_C in sub-population C. We can solve this system using the method of characteristics—a method that reduces our first-order linear PDE to a family of ODEs.

2.1.2 | Deriving a renewal equation and the time-varying reproduction number

To solve the system of PDEs, Equations (2.1–2.6), we use (i) the characteristic form of the infected mosquito population, (ii) the boundary condition on the mosquito population, Equation (2.5) and (iii) the characteristic form of the infected human population to derive the following renewal equation (see Appendix B):

$$E(t,0)=\int_0^{t}\int_0^{t-a_M} b_{ME}(t,a_M)e^{-\mu a_M}b_{EM}(t-a_M,a_E)E(t-a_M-a_E,0)da_E da_M, \tag{2.7}$$

where we have ignored initial conditions f_E and f_M Equations (2.4) and (2.6) and assumed that the epidemic is well-established, allowing us to focus on longer-term dynamics (such that $t\gg a_M$ and $t\gg a_E$).

Then, we seek a solution of the form: $E(t,a_E)=p(a_E)e^{\gamma t}$. This solution states that the age distribution of infected humans is altered by a factor which grows or decays with time depending on whether $\gamma>0$ or $\gamma<0$, respectively. Substituting the expression into Equation (2.1), we deduce that $p(a_E)=p(0)e^{-\gamma a_E}$. From Equation (2.7), we have

$$\phi(\gamma):=\int_0^{t}\int_0^{t-a_M} b_{ME}(t,a_M)e^{-\mu a_M}b_{EM}(t-a_M,a_E)e^{-\gamma(a_E+a_M)}da_E da_M. \tag{2.8}$$

This expression is defined for each calendar time t. From Equation (2.8), we define an instantaneous growth rate $r_t:=\{\gamma \text{ such that } \phi(\gamma)=1\}$, which is unique as $\phi(\gamma)$ is a monotonically decreasing function of γ. This instantaneous growth rate for human infections provides a measure of the long-run behaviour of human infections, should the conditions affecting human transmission at time t remain the same. Our model-based definition of r_t does not account for transient behaviour (which is likely important in stochastic, early outbreak stages; Smith et al., 2014) and should not be confused with empirical approaches (e.g. Pellis et al., 2022) that estimate an instantaneous growth rate r_t from case/prevalence data, often using a smoothing window approach (Parag et al., 2022). As $\phi(\gamma)$ is a monotonically decreasing function of γ, $\phi(0)$ is the critical threshold for epidemic growth. This is because $r_t>0$ when $\phi(0)>1$ and $r_t<0$ when $\phi(0)<1$ (see Figure 2a,b).

So, we define $R(t)$ as:

$$R(t):=\phi(0)=\int_0^{t}\int_0^{t-a_M} b_{ME}(t,a_M)e^{-\mu a_M}b_{EM}(t-a_M,a_E)da_E da_M. \tag{2.9}$$

$R(t)$ defines a time-varying human-to-human reproduction number because our renewal equation for the newly infected human population (Equation 2.7) has only a single birth state (for new human infections), and so the corresponding next-generation operator (Diekmann & Heesterbeek, 2000), describing the number of new human infections produced by previously infected individuals, is:

$$\mathbb{K}:=\int_0^{t}\int_0^{t-a_M} b_{ME}(t,a_M)e^{-\mu a_M}b_{EM}(t-a_M,a_E)da_E da_M.$$

The time-varying reproduction number $R(t)$ is the largest (and only) absolute eigenvalue of $\mathbb{K}$. So, Equation (2.9) defines the instantaneous human-to-human reproduction number $R(t)$ as, relying on only information up to time t, it is the average number of secondary human infections that an infected human would generate over their infected lifetime if the current conditions remained the same. Here, when discussing current conditions, these are the conditions that currently affect infection of humans—conditions which are determined by the historical conditions experienced for the previous stages of the transmission cycle.

2.1.3 | A closer look at R_0 and r

If the birth processes $b_{ME}(t,a_M)$ and $b_{EM}(t,a_E)$ do not change over calendar time, and we take the limit as $t\to\infty$, then Equation (2.9) defines

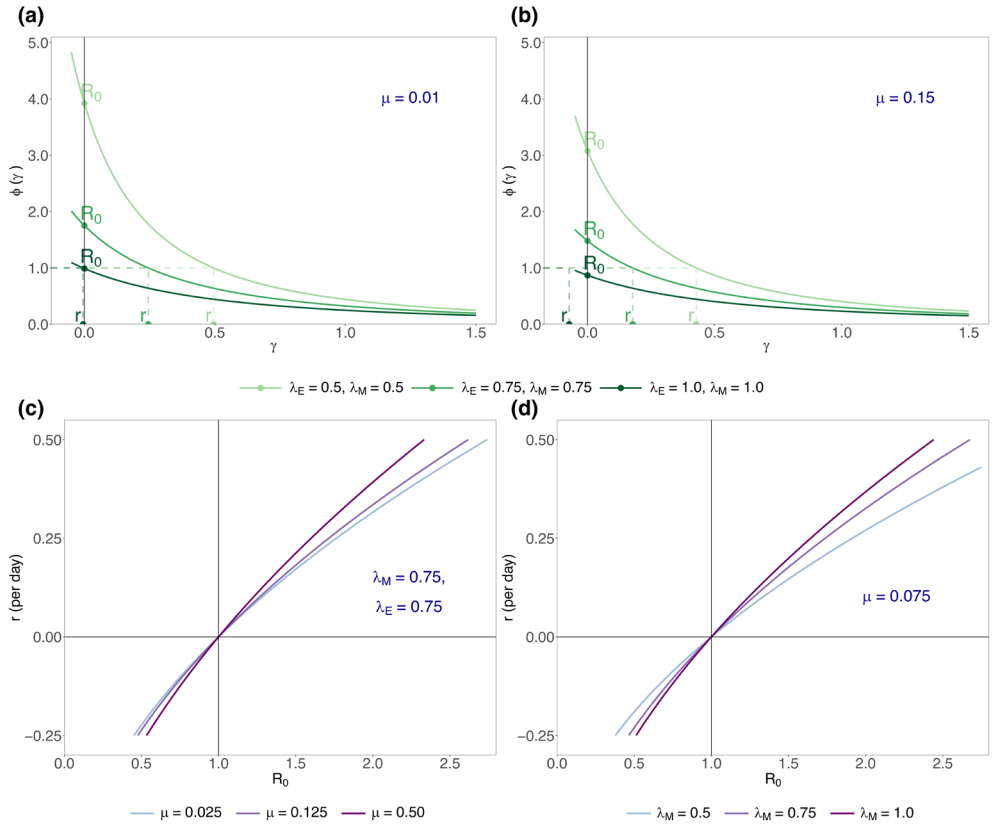

FIGURE 2 R_0 and r under different mosquito-human traits for the modelling framework described by Equations (2.1–2.5). We assume $b_{EM}(t,a_E)=\exp(-\lambda_E a_E)$ and $b_{ME}(t,a_M)=\exp(-\lambda_M a_M)$. These assume that the birth processes decline only with time since infection. Panels (a) and (b): We visualise how R_0 and r are derived for varying infection rates (λ_M and λ_E for the production of infected humans and mosquitoes respectively) and mosquito death rates (μ). $r=\{\gamma \text{ such that } \phi(\gamma)=1\}$ and $R_0=\phi(0)$. Panels (c) and (d): The relationship between r and R_0, (Equation B.25) in Appendix B.4, is traced out for the modelling framework under three different mosquito death rates μ (left) and three fixed different mosquito infection rates λ_M (right). These figures would be visualisations of the relationship between $R(t)$ and r_t, at each calendar time t, if we had not assumed time-independent birth processes $b_{EM}(t,a_E)$ and $b_{ME}(t,a_M)$.

a basic reproduction number R_0 with a corresponding intrinsic growth rate r. We can use simple exponential forms for birth processes, $b_{ME}(t,a_M)=\exp(-\lambda_M a_M)$ and $b_{EM}(t,a_E)=\exp(-\lambda_E a_E)$, to obtain analytical results. We illustrate these derivations in Figure 2 for R_0 and r (see also Appendix B.4 for further details). The figure shows the familiar threshold relationship between R_0 and r i.e. $R_0>1$ when $r>0$. Also, faster declines in infection rates (from time since infection) and higher mosquito death rates both increase the exponential growth rate r for a fixed $R_0>1$. Intuitively, this is because if, for example, mosquitoes have shorter lives, yet bequeath the same number of infections over their infected lifetime, then the epidemic must be growing faster. The figure also demonstrates that interventions which reduce R_0 by a fixed amount cause smaller changes in r as R_0 increases.

2.1.4 | Instantaneous kernels and generation time distributions

$R(t)$ is often written in terms of (i) the instantaneous kernel or (ii) the generation time distribution and the instantaneous growth rate. To obtain this form, we write Equation (2.9) as

$$R(t)=\int_0^t\int_0^{t-a_M} b_{ME}(t,a_M)e^{-\mu a_M}b_{EM}(t-a_M,a_E)da_E da_M,$$
$$=\int_0^t\int_0^{t-a_M} K(t,a_M,a_E)da_E da_M, \tag{2.10}$$

which suggests defining a two-dimensional probability density, at calendar time t, for the generation time $g(t,a_M,a_E):=K(t,a_M,a_E)/R(t)$. This distribution controls the times between the primary and secondary human infections. As required for a generation time distribution, it is the normalised version of the instantaneous kernel $K(t,a_M,a_E)$ (Metz & Diekmann, 1986; Park et al., 2022; Wallinga & Lipsitch, 2007). The kernel defines the average rate at which secondary human infections are generated at time t by (i) a mosquito infected a_M time units ago and (ii) a human that was of infection age a_E at time $t-a_M$. So, $g(t,a_M,a_E)$ defines the relative contributions to secondary human infections at time t of a mosquito of infection age a_M at time t that was itself infected by a human of age a_E at time $t-a_M$. This is similar to existing interpretations for directly transmitted infectious diseases, as the expected relative contribution to the

force of infection by a human infected a $\tau = a_E + a_M$ time units ago (Breda et al., 2012; Park et al., 2022).

As in the setting of directly transmitted infectious diseases (Park et al., 2022), both the $g(t, a_M, a_E)$ and $R(t)$ are (counterfactual) instantaneous measures of relative contributions to human infections and of time-varying transmissibility respectively; these are counterfactual because they are defined using historical conditions under assumptions of conditions affecting human transmission remaining the same as at time t.

Using Equations (2.8) and (2.10), we have:

$$\frac{1}{R(t)} = \int_0^t \int_0^{t-a_M} g(t, a_M, a_E) e^{-r_t(a_E+a_M)} da_E da_M, \tag{2.11}$$

which shows how $g(t, a_M, a_E)$ controls the relationship between r_t and $R(t)$ (Figure 2c,d).

Our renewal equation for the newly infected human population can now be written in terms of the generation time distribution and the instantaneous reproduction number:

$$E(t,0) = \int_0^t \int_0^{t-a_M} K(t, a_M, a_E) E(t - a_M - a_E, 0) da_E da_M, \tag{2.12}$$

$$= R(t) \int_0^t \int_0^{t-a_M} g(t, a_M, a_E) E(t - a_M - a_E, 0) da_E da_M. \tag{2.13}$$

The renewal equation features $E(t - a_M - a_E, 0)$, the humans previously infected at time $t - a_M - a_E$. The corresponding generation time distribution is described by $g(t, a_M, a_E)$ and is calculated using intermediate calendar times when generation events occur in the transmission cycle (see Equation 2.20 below). We define a generation event to occur when a new individual is generated (or born) in a sub-population.

The key to our generation time distribution is that it depends on (i) the stages of the transmission cycle and (ii) the calendar times at which they begin—see Figure 1c for a visualisation.

2.1.5 | Between-stage reproduction numbers

We can also define a reproduction number between stages, which gives the average number of infected humans generated per infected mosquito:

$$R_{ME}(t) := \int_0^t b_{ME}(t, a_M) e^{-\mu a_M} da_M,$$
$$\beta_{ME}(t, a_M) := \frac{b_{ME}(t, a_M) e^{-\mu a_M}}{R_{ME}(t)}, \tag{2.14}$$

where $1 = \int_0^t \beta_{ME}(t, a_M) da_M$ and $\beta_{ME}(t, a_M)$ is the probability density, at calendar time t, of the generation time from infected mosquitoes to infected humans. $\beta_{ME}(t, a_M)$ is defined by normalising the instantaneous kernel between stages (i.e. the average rate at which human infections are generated at time t by a mosquito infected a_M time units ago). So, $\beta_{ME}(t, a_M)$ defines the relative contribution of mosquitoes of age a_M to human infections at time t.

We also produce a reproduction number for the human-to-mosquito component of the dynamics:

$$R_{EM}(t - a_M) := \int_0^{t-a_M} b_{EM}(t - a_M, a_E) da_E,$$
$$\beta_{EM}(t - a_M, a_E) := \frac{b_{EM}(t - a_M, a_E)}{R_{EM}(t - a_M)}, \tag{2.15}$$

where $1 = \int_0^{t-a_M} \beta_{EM}(t - a_M, a_E) da_E$ and $\beta_{EM}(t - a_M, a_E)$ is the probability density, at calendar time $t - a_M$, of the generation time from infected humans to infected mosquitoes. So, $\beta_{EM}(t - a_M, a_E)$ describes the relative contributions of infected humans (to the generation of newly infected mosquitoes) that were of age a_E at time $t - a_M$.

Equations (2.14–2.15) collectively result in a modification of Equation (2.7) to

$$E(t,0) = R_{ME}(t) \int_0^t \beta_{ME}(t, a_M) R_{EM}(t - a_M) \int_0^{t-a_M} \beta_{EM}(t - a_M, a_E) E(t - a_M - a_E, 0) da_E da_M, \tag{2.16}$$

and also of Equation (2.9) to

$$R(t) = R_{ME}(t) \int_0^t \beta_{ME}(t, a_M) R_{EM}(t - a_M) da_M$$
$$= R_{ME}(t) \mathbb{E}_{ME}[R_{EM}(t - a_M)], \tag{2.17}$$

where $\mathbb{E}_{ME}[X(t - a_M)] := \int_0^{t-a_M} X(t - a_M) \beta_{ME}(t, a_M) da_M$. This defines the reproduction number as expectations across the between-stage reproduction numbers. Equation (2.17) is similar to a geometric average of the between-stage reproduction numbers for an entire system (e.g. Brouwer, 2022; Funk et al., 2016; Keeling et al., 2008), and here we define a human-to-human reproduction number $R(t)$ which requires that a new human infection requires a two-stage process.

2.1.6 | Relation to existing renewal equation frameworks

Our integral equation, Equation (2.13), can be related to the ubiquitous renewal equation frameworks for directly transmitted infectious diseases (see Appendix B.3).

Since $t - (a_M + a_E)$ occurs in our renewal equation, Equation (2.13), we can define a new variable, $\tau = a_E + a_M$, measuring the overall delay between primary and secondary human infections. By a change of variables and an integration step, we produce a one-dimensional renewal equation:

$$E(t,0) = R(t) \int_0^t w(t, \tau) E(t - \tau, 0) d\tau, \tag{2.18}$$

where $w(t,\tau) \coloneqq \int_0^\tau g(t,\tau-a_E,a_E)da_E$.

If we assume the generation time distribution is constant over calendar time, (i.e. $g(t,a_M,a_E)=g(a_M,a_E),\forall t$), we recover the familiar renewal equation (Abbott et al., 2020; Cori et al., 2013; Fraser, 2007; Parag, 2021), as in Equation (1.1):

$$E(t,0)=R(t)\int_0^t w(\tau)E(t-\tau,0)d\tau. \tag{2.19}$$

Assuming a constant generation time distribution over calendar time means that the ratio

$$\begin{aligned} g(t,a_M,a_E) &= \frac{K(t,a_M,a_E)}{R(t)} \\ &= \frac{b_{ME}(t,a_M)e^{-\mu a_M}b_{EM}(t-a_M,a_E)}{\int_0^t\int_0^{t-a_M} b_{ME}(t,a_M)e^{-\mu a_M}b_{EM}(t-a_M,a_E)da_E da_M}, \end{aligned} \tag{2.20}$$

is fixed over calendar time (t). So, this typically implicit modelling assumption means that the relative expected contribution to secondary human infections of each pair of ages (i.e. times-in-states (a_M,a_E)) is constant over the course of an outbreak. This means $K(t,a_M,a_E)$ scales linearly over calendar time t with the expected overall number of new infections generated (across all age combinations of sub-populations) per initially infected human, $R(t)$.

The assumption may be unrealistic for dengue or any vector-borne disease with a multi-stage transmission cycle. For example, higher temperatures may reduce the extrinsic incubation period of dengue (Chan & Johansson, 2012), and/or changes in the host and vector population sizes (which may themselves have temperature and precipitation dependencies) could alter the distribution of times between generation events.

Equation (2.19) formalises the relationship between our framework and existing renewal equations (used in e.g. Abbott et al., 2020; Cori et al., 2013; Fraser, 2007; Parag, 2021). The existing renewal equations are a special case of our general framework with an additional assumption of a time-invariant generation time distribution.

2.2 | Exposure-and-infection-age-structured populations of humans and mosquitoes

2.2.1 | Modelling framework

We now extend the above framework to a transmission cycle with four sub-populations which includes exposed and infectious sub-populations in the host and vector populations. This structure accounts for the intrinsic and extrinsic latent periods (i.e. the time taken from mosquito bite to the host or mosquito respectively becoming infectious). The system, consisting of densities of an exposed (E) and infectious (I) human population, and an exposed (W) and infectious (V) mosquito population, is subject to the following conservation equations (e.g. Chapter 1.7 in Murray, 2002):

$$\frac{\partial E}{\partial t}+\frac{\partial E}{\partial a_E}=-b_{EI}(t,a_E)E(t,a_E), \tag{2.21}$$

$$\frac{\partial I}{\partial t}+\frac{\partial I}{\partial a_I}=0, \tag{2.22}$$

$$\frac{\partial W}{\partial t}+\frac{\partial W}{\partial a_W}=-b_{WV}(t,a_W)W(t,a_W)-\mu W(t,a_W), \tag{2.23}$$

$$\frac{\partial V}{\partial t}+\frac{\partial V}{\partial a_V}=-\mu V(t,a_V), \tag{2.24}$$

where again each $b_{CD}(t,a_C)\geq 0$ is a time- and age-dependent birth function that represents the rate at which new individuals in sub-population D are generated at calendar time t by an individual of age a_C in sub-population C. $\mu \geq 0$ is the mosquito death rate for both exposed and infectious mosquitoes, which we assume is age- and infection-status-independent (Lambert et al., 2022).

We close the system with the following initial and boundary conditions.

$$E(t,0)=\int_0^\infty b_{VE}(t,a_V)V(t,a_V)da_V, \tag{2.25}$$

$$E(0,a_E)=f_E(a_E), \tag{2.26}$$

$$I(t,0)=\int_0^\infty b_{EI}(t,a_E)E(t,a_E)da_E, \tag{2.27}$$

$$I(0,a_I)=f_I(a_I), \tag{2.28}$$

$$W(t,0)=\int_0^\infty b_{IW}(t,a_I)I(t,a_I)da_I, \tag{2.29}$$

$$W(0,a_W)=f_W(a_W), \tag{2.30}$$

$$V(t,0)=\int_0^\infty b_{WV}(t,a_W)W(t,a_W)da_W, \tag{2.31}$$

$$V(0,a_V)=f_V(a_V). \tag{2.32}$$

where $f_E(a_E), f_I(a_I), f_W(a_W)$, and $f_V(a_V)$ are the initial densities for the exposed human, infectious human, exposed mosquito and infectious mosquito populations respectively. Note that $b_{VE}(t,a_V)$ and $b_{IW}(t,a_I)$ represent the processes by which new infections occur in humans and mosquitoes respectively, while $b_{EI}(t,a_I)$ and $b_{WV}(t,a_V)$ represent the processes by which infected humans and mosquitoes become

infectious. We consider possible functional forms for these birth processes in Equation (3.1).

An intermediate system with three sub-populations is provided in Appendix C, and additional derivation details for this four-compartment framework are provided in Appendix D.

2.2.2 | Deriving a renewal equation and the time-varying reproduction number

We can derive the following renewal equation for newly infected humans:

$$E(t,0)=\int_0^t\int_0^{t-a_V}\int_0^{t-a_V-a_W}\int_0^{t-a_V-a_W-a_I} b_{VE}(t,a_V)b_{WV}(t-a_V,a_W)b_{IW}(t-a_V-a_W,a_I)\cdot b_{EI}(t-a_V-a_W-a_I,a_E)e^{-\mu a_V}e^{-\int_0^{a_W} b_{WV}(t-a_V-a_W+r,r)dr-\mu a_W}\cdot E(t-a_V-a_W-a_I-a_E,0)e^{-\int_0^{a_E} b_{EI}(t-a_V-a_W-a_I-a_E+s,s)ds}da_E da_I da_W da_V, \tag{2.33}$$

where we have again assumed long-term epidemic dynamics (such that $t \gg a_V$, $t \gg a_W$ and $t \gg a_I$, $t \gg a_E$). We again try a separable solution (to derive analytical results) of the form $E(t,a_E)=p(a_E)e^{\gamma t}$. To have a separable form for Equation (2.33), we must assume that $b_{EI}(t,a_E)=b_{EI}(a_E)\,\forall\, t$. This amounts to assuming that the rate at which an exposed individual becomes infectious is independent of calendar time (t) and depends only on time since exposure (a_E). Then, we can derive a formula for the time-varying human-to-human reproduction number:

$$\begin{aligned}R(t)&=\int_0^t\int_0^{t-a_V}\int_0^{t-a_V-a_W}\int_0^{t-a_V-a_W-a_I} b_{VE}(t,a_V)b_{WV}(t-a_V,a_W)b_{IW}(t-a_V-a_W,a_I)\cdot b_{EI}(a_E)e^{-\mu a_V}e^{-\int_0^{a_W} b_{WV}(t-a_V-a_W+r,r)dr-\mu a_W}e^{-\int_0^{a_E} b_{EI}(s)ds}\\&\qquad da_E da_I da_W da_V\\&=\int_0^t\int_0^{t-a_V}\int_0^{t-a_V-a_W}\int_0^{t-a_V-a_W-a_I} K(t,a_E,a_I,a_W,a_V)da_E da_I da_W da_V,\end{aligned} \tag{2.34}$$

which suggests the following definition of a four-dimensional probability density

$$g(t,a_E,a_I,a_W,a_V) \coloneqq \frac{K(t,a_E,a_I,a_W,a_V)}{R(t)}, \tag{2.35}$$

for the generation time at calendar time t, derived by normalising the instantaneous kernel.

Again, the time-varying reproduction number $R(t)$ is an instantaneous reproduction number for the infected human population, and defines the expected number of secondary human infections produced at calendar time t by an infected human, if the conditions that affect human infections at time t were to remain the same. The instantaneous kernel $K(t,a_E,a_I,a_W,a_V)$ is the expected rate at which secondary human infections are generated at calendar time t across individuals of stage-specific ages (a_E,a_I,a_W,a_V); these ages are the times-since-state-entry at the calendar times when each sub-population plays their role in the transmission cycle.

At each calendar time t, the generation time distribution describes the relative contributions to the current number of new human infections generated by previously exposed humans, previously infectious humans, previously exposed mosquitoes and currently infectious mosquitoes of specific ages (i.e. the times spent in compartments until each population plays their role in generation events—see Figure 1c).

We can then rewrite Equation (2.33) to produce a more familiar renewal equation:

$$E(t,0)=R(t)\int_0^t\int_0^{t-a_V}\int_0^{t-a_V-a_W}\int_0^{t-a_V-a_W-a_I} g(t,a_E,a_I,a_W,a_V)\cdot E(t-a_V-a_W-a_I-a_E,0)da_E da_I da_W da_V. \tag{2.36}$$

2.2.3 | Between-stage reproduction numbers

As before, we can define reproduction numbers and generation time distributions between stages (see Appendix D.3). This allows us to rewrite Equation (2.34) as an expectation of reproduction numbers across stages of the transmission cycle:

$$R(t)=R_{VE}(t)\mathbb{E}_{VE}\left[R_{WV}(t-a_V)\mathbb{E}_{WV}\left[R_{IW}(t-a_V-a_W)\mathbb{E}_{IW}\left[R_{EI}(t-a_V-a_W-a_I)\right]\right]\right], \tag{2.37}$$

where each $\mathbb{E}_{AB}\left[R_{CA}(t-a_A)\right] \coloneqq \int_0^{t-a_A} R_{CA}(t-a_A)\beta_{AB}(t,a_A)da_A$ and each $R_{CA}(t)$ defines the average number of individuals in sub-population A produced by an individual in sub-population C if conditions were to remain the same as at time t. The between-stage reproduction numbers are evaluated with upper limits determined by the calendar times at which the subsequent stage of the transmission cycle begins. The expectations are taken with respect to the generation time distribution (β_{AB}) between stages of the next stage of the transmission cycle. The generation time distributions between stages are evaluated using ages of the sub-populations at the calendar times at which onward generation events in the transmission cycle occur (see Figure 1c: a_V at time t, a_W at time $t-a_V$ and a_I at time $t-a_V-a_W$).

2.2.4 | Application to simulated and real-world data

We now consider a numerical application, where our aim was to investigate the importance of tracking the calendar times of the transmission cycle when estimating the generation time distribution. For simplicity, this example is not a full exposition of our mechanistic framework Equations (2.21–2.32); it only uses the assumptions governing how stage durations depend on temperature outlined by Siraj et al. (2017) (see Appendix D.4), and does not consider estimating

$R(t)$ (see Section 3). All code and data used in these applications are contained in a Zenodo repository (Mills, 2025).

We used daily mean temperature data from Ang Mo Kio (a town in Singapore), Foz do Iguaçu (a city in Brazil) and São João do Tauape (a neighbourhood in the city of Fortaleza, Brazil), as well as simulated daily temperature data (Hersbach et al., 2020; Meteorological Service Singapore, 2024). Locations were selected due to known circulation of dengue viruses. We investigated differences in generation time distributions when using a stage-specific approach versus an existing one (see Siraj et al., 2017) which ignores the calendar times of the stages of the transmission cycle. For both approaches, we estimated the generation time distribution assuming the four-stage transmission cycle (Figure 1a) and Monte Carlo sampling (see Appendix D.4). Our Monte Carlo procedure for both approaches provides samples of $\tau = a_E + a_I + a_W + a_V$, the time between primary and secondary human infections (which follows the distribution with density $w(t,\tau)$). To produce a sample of τ, we sample a_E, a_I, a_W and a_V from their assumed between-stage distributions.

For (i) the existing approach which ignores the calendar times at which transitions between stages of the transmission cycle occur, the generation time distribution is changed every day based on the temperature observed that day. To obtain samples from $w(t,\tau)$, we sampled $a_E^i \sim \beta_{EI}(t,a_E)$, $a_I^i \sim \beta_{IW}(t,a_W)$, $a_W^i \sim \beta_{WV}(t,a_W)$ and $a_V^i \sim \beta_{VE}(t,a_V)$, based on the temperature observed at the same calendar time t. This Monte Carlo sampling procedure gives a single sample $\tau^i = a_E^i + a_I^i + a_W^i + a_V^i$ from $w(t,\tau)$, and we repeated this procedure to obtain 2000 samples from $w(t,\tau)$.

For (ii) our stage-specific approach, the generation time distribution was based on temperatures observed for calendar times when the estimated generation events occurred. Both approaches have the same assumptions for temperature effects on stage durations, but our stage-specific approach uses between-stage distributions based on current *and* historical temperatures. For this stage-specific approach, we used the sampling distributions (between stages) outlined by Siraj et al. (2017) in the following way: we sampled $a_V^i \sim \beta_{VE}(t,a_V)$, $a_W^i \sim \beta_{WV}(t-a_V^i,a_W)$, $a_I^i \sim \beta_{IW}(t-a_V^i-a_W^i,a_W)$ and $a_E^i \sim \beta_{EI}(t-a_V^i-a_W^i-a_I^i,a_E)$. This Monte Carlo sampling procedure gives a single sample $\tau^i = a_E^i + a_I^i + a_W^i + a_V^i$ from $w(t,\tau)$. Note a sample for a_V is based on the between-stage distribution at time t, whereas samples of a_I, a_W and a_E are based on the between-stage distributions at times before time t. We repeated this procedure to obtain 2000 samples from $w(t,\tau)$.

We quantified the difference between the existing and stage-specific approaches at each time point using the Kullback–Leibler (KL) divergence, and visualised the cumulative KL divergence to capture the total difference over time.

We investigated short time periods (8 weeks, Figure 3a–c) where dengue was likely to circulate and longer time periods (an entire year, Figure 3d,e) where dengue was less likely to circulate (due to winter temperatures). To illustrate the effects of a volatile environment, our simulated daily temperature data was based on a Gaussian random walk (with noise $\epsilon_t \sim N(0,4)$, and reflecting boundaries at 20 and 45°C).

For the 8-week period, in the applications to real-world temperature data (Figure 3a,b, Figures S1–S4), there were similar trends in the estimated generation time distributions across the two methods. However, the higher variability in the simulated temperature data (Figure 3c, Figures S5 and S6) resulted in notable differences in the evolution of the generation time distributions, as indicated by the cumulative KL divergence over the 8-week period. For the year-long period, in São João do Tauape (Figure 3d), the generation time distribution from both methods did not fluctuate wildly over calendar time since the temperature conditions were relatively stable temperature conditions. In contrast, the volatile temperatures observed in the city of Foz do Iguaçu (Figure 3e) resulted in extreme, long generation times. These results hint that at lower temperatures, transmission could be slowed by temperature-mediated effects. However, these estimates are the result of extrapolating laboratory results directly into the field, which likely overstates the impact of temperature on transmission (see Section 3). Changes in temperature are also likely correlated with rainfall amounts, resulting in changes in the mosquito population dynamics which may dominate the temperature effects.

Across the five settings (Figure 3a–e), the stage-specific approach acted like a smoothed average versus the existing approach as the generation time distribution was based on temperatures observed throughout the transmission cycle. These differences are most pronounced in the simulated setting (Figure 3c) and Foz do Iguaçu (Figure 3e) when temperatures varied more widely, and the cumulative KL divergence was substantially larger in these settings versus analogous settings with less temperature variability.

3 | DISCUSSION

Transmission of mosquito-borne pathogens is sensitive to environmental fluctuations, particularly to changes in temperature and elements of their transmission cycle respond differently to these variations (Chan & Johansson, 2012; Huber et al., 2018; Monteiro et al., 2019; Mordecai et al., 2017). This temporal variation means that there is no fixed distribution governing the time it takes one human infection to cause (through the vector) a subsequent human infection. This creates issues for traditional renewal frameworks which assume that this so-called generation time distribution is fixed. Here, we derive from first principles a renewal equation that applies to mosquito-borne diseases, which naturally accounts for temporal variation in each element of the transmission cycle. Time-varying reproduction numbers and epidemic growth rates emerge from our renewal equation framework, and this provides a theoretically grounded basis for estimating these important metrics of pathogen transmission rates.

Our empirical results indicate that, under the assumption of previously estimated temperature dependencies (for times between stages of the transmission cycle; Chan & Johansson, 2012; Siraj et al., 2017), the generation time distribution is likely to be transient, changing during a mosquito-borne disease outbreak in response to

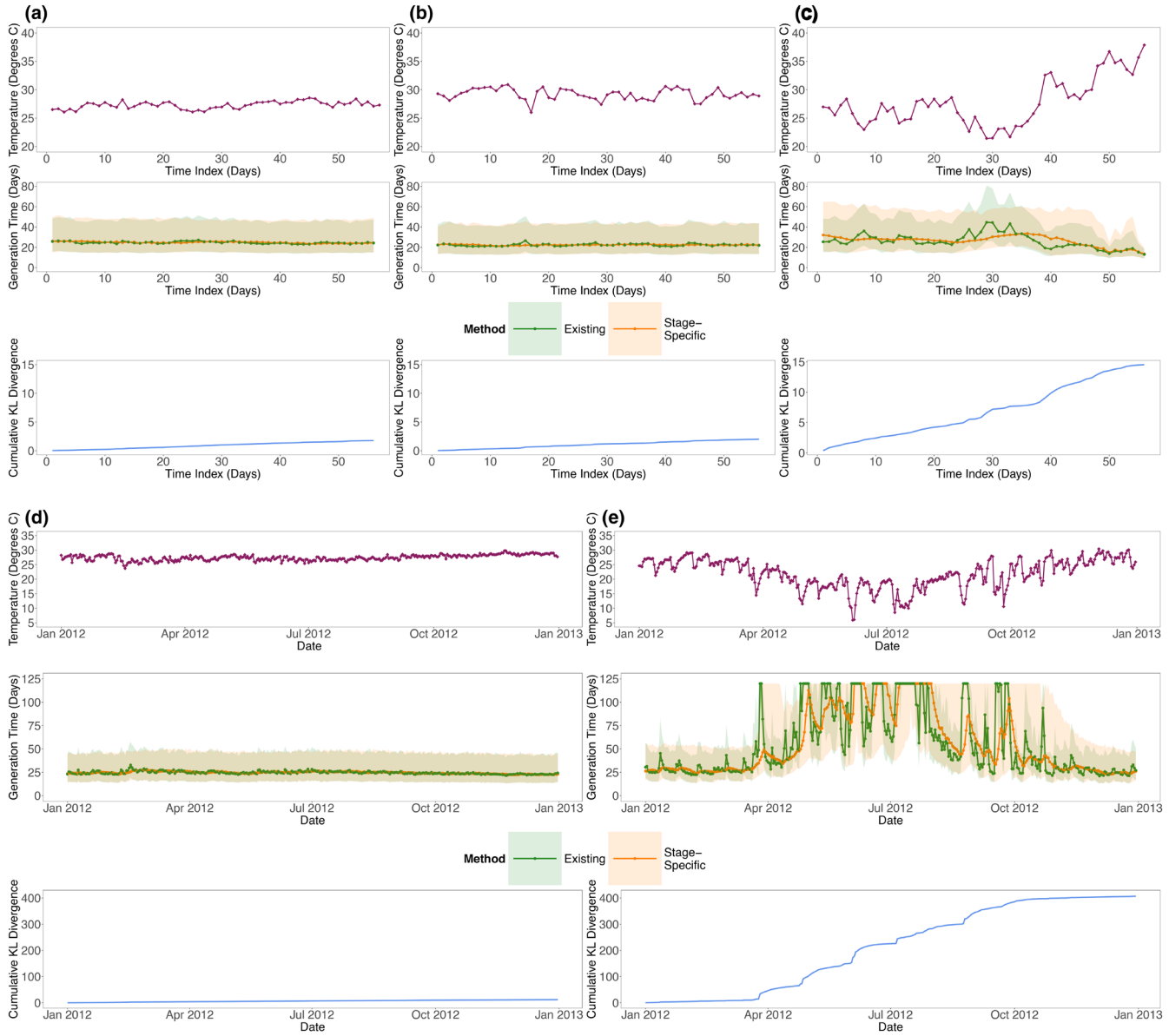

FIGURE 3 Generation time (GT) distributions under temperature-dependent conditions: For the four-stage transmission cycle of dengue, we illustrate GT distributions at different calendar times. In these toy examples, the distributions were estimated using Monte Carlo sampling (see Appendix D.4). We assumed temperature-dependent GT distributions and used daily temperature data and either a stage-specific (orange) or an existing (green) approach. The filled circles indicate the medians of the 2000 Monte Carlo samples, and the shaded regions indicate the central 95% intervals of the samples. For the *stage-specific* approach, the GT distribution was based on temperatures observed for calendar times when the estimated generation events occurred (i.e. depending on current and historical temperatures). The *existing* approach ignores the calendar times at which transitions between stages of the transmission cycle occur, and the GT distribution is changed every day based on the temperature observed that day. For both approaches, we assumed the same temperature effects on times between transmission cycle stages (which were outlined by Siraj et al., 2017, see Appendix D.4). GT distributions were estimated using daily mean temperature (purple) data for (a) Ang Mo Kio, Singapore (December 2023 to June 2024), (b) São João do Tauape, Brazil (November 2011 to May 2012), (c) a simulated environment (using a Gaussian random walk with noise $\epsilon_t \sim N(0,4)$, and maximum and minima of 20 and 45°C respectively), (d) São João do Tauape, Brazil (January 2012 to December 2012) and (e) Foz do Iguaçu, Brazil (January 2012 to December 2012) (Hersbach et al., 2020; Meteorological Service Singapore, 2024). The upper plots, (a–c), show GT distributions over 56 days (8 weeks), while the lower plots, (d, e), show GT distributions over 1 year. We used different *y*-axes for the plots in panels (a–c) versus (d, e) for legibility. For panel (e), we bounded the maximum GT delay (*y*-axis) at 120 days, consistent with the approach taken by Siraj et al. (2017). For each of (a–e), we measured the difference between the existing and stage-specific approach using Kullback–Leibler (KL) divergence, and plotted the cumulative KL divergence over time.

varying environmental conditions. Future empirical work may look at embedding other environmental, biological and demographic conditions (beyond temperature) into the time-varying components of the birth processes which control the generation time distribution (see below, Equation 3.1). However, our results indicate that this distribution depends on both current and historical conditions. This dependence on history is because, for transmission to occur, a full sequence of stages of the transmission cycle must be completed and each of these stages could be exposed to different conditions. Our generation time distribution at a given time then represents the uncertainty in the typical time between parent and daughter infections if conditions were as they were historically. The mechanistic, history-dependent nature of our generation time distribution contrasts with existing less mechanistic approaches which more heuristically allow the generation time distribution to change in response to only current conditions (Siraj et al., 2017). Our empirical results (albeit only using previously documented temperature dependencies for times between stages of transmission; Chan & Johansson, 2012; Siraj et al., 2017) hint that our approach predicts less temporal variation in the generation time distribution than approaches based only on current conditions. This is because the dependence on historical conditions likely acts to smooth its variation over time. More generally, beyond our simplified numerical application, our theory for the generation time distribution also differs from other less mechanistic approaches (Codeço et al., 2018; Ong et al., 2022; Scire et al., 2023). These approaches either assume time-invariant generation time distributions or do not directly normalise the relative contributions of different sub-population ages (i.e. the instantaneous kernel), and instead can only respond to observed temperature values—ignoring other sources of temporal variation for elements of the transmission cycle.

Ours and other approaches to modelling mosquito-borne pathogen transmission depend on assumptions about how elements of the pathogen and mosquito lifecycle respond to environmental conditions, and these are largely drawn from laboratory studies. Many such studies have shown that variations in temperature substantially affect the time spent in particular lifecycle stages. For malaria, Zika, dengue and a range of arboviruses, the time taken for an infected mosquito to become infectious is hastened by higher environmental temperatures in the laboratory. Mosquitoes also die more rapidly at elevated laboratory temperatures (Chan & Johansson, 2012; Mordecai et al., 2019; Yang et al., 2009). These laboratory studies underpin a wide range of modelling studies that extrapolate how mosquito-borne pathogen transmission may respond to changes in temperature (e.g. Chen et al., 2024; Siraj et al., 2017). However, more work is required to understand whether these results from laboratory studies hold in the wild: mosquitoes, like all insects, are cold-blooded and rely on their environment to thermoregulate, meaning they adjust their behaviour in response to changes in environmental conditions. Since the laboratory mosquitoes are limited in their environment, they are likely limited in their ability to respond to temperature changes. Laboratory mosquitoes are often highly inbred, which may also make them more fragile to temperature changes. This means that laboratory studies likely overstate the impacts of temperature on disease transmission, and field or semi-field studies are crucial.

Despite recent advances in understanding temperature-dependent transmission (Mordecai et al., 2017; Shocket et al., 2020; Tesla et al., 2018), we still do not have a comprehensive understanding of whether results from laboratory studies will transfer to the field. This is essential as the incidence and distribution of many mosquito-borne diseases such as dengue continue to rise in the climate crisis, and model-based projections under different climate change scenarios are often underpinned by these estimated temperature dependencies (Dennington et al., 2025; Mordecai et al., 2019). Understanding how mosquitoes respond (and the shape of the generation time distribution) to increasing future climatic variability will be important for future projections of dengue burden and could be achieved by embedding these projections in our model. Despite our simplifying numerical application, there are many environmental and biological factors other than temperature that may affect the transmission of pathogens. For example, the rate at which mosquitoes become infected and infect humans depends on demography—the population sizes of mosquitoes and susceptible humans (see Equation 3.1). Mosquito population dynamics are driven by the availability of water sources due to the dependence of the initial mosquito life stages on these. So, rainfall also affects the rate of pathogen transmission, although this aspect is typically ignored in existing renewal-type models of mosquito-borne infection transmission. Our model considers pathogen dynamics and only the dynamics of infected mosquitoes, and we could straightforwardly link it to the overall mosquito population dynamics by allowing the birth rate of infections in either humans or mosquitoes to depend on these. Modelling how mosquito population dynamics depend on both temperature and rainfall would then allow forward projections of pathogen transmission rates to be made.

Incorporating these dependencies (beyond temperature effects) and inferring $R(t)$ (e.g. alongside case data and/or densities of human and mosquito populations) will depend on parameterising the time-varying processes of Equations (2.21–2.32), which control both the generation time distribution and $R(t)$. These are key to extending our numerical application beyond estimating the generation time distribution. As an example, we could have:

$$
\begin{aligned}
b_{EI}(t,a_E) &= \lambda^{E}_{\text{Latent}}(a_E)\\
b_{IW}(t,a_I) = \frac{b(t)}{N^H(t)}\cdot S^M(t)\cdot p_{WI} &= \frac{b(t)}{N^H(t)}\cdot\left(N^M(t)-\int_0^{\infty} W(t,a_W)da_W-\int_0^{\infty} V(t,a_V)da_V\right)\cdot p_{WI}\\
b_{WV}(t,a_W) &= \lambda^{W}_{\text{Latent}}(a_W)\\
b_{VE}(t,a_V) = b(t)\cdot\frac{S^H(t)}{N^H(t)}\cdot p_{EV} &= b(t)\left(N^H(t)-\int_0^{t} E(t,a_E)da_E-\int_0^{t} I(t,a_I)da_I\right)/N^H(t)\cdot p_{EV}
\end{aligned}
\tag{3.1}
$$

where $\lambda^{E}_{\text{Latent}}(a_E)$ and $\lambda^{W}_{\text{Latent}}(a_W)$ denote the rates at which latent periods end for infected humans and mosquitoes respectively, $N^H(t)$ and $N^M(t)$ denote the total human and mosquito populations, $S^H(t)$ and

$S^M(t)$ denote the susceptible human and mosquito population counts, p_{WI} and p_{EV} denote the probability of mosquito and human infection upon infectious bite respectively, and $b(t)$ denotes the rate at which a mosquito bites a human. Equation (3.1) relies on counts for mosquito and human sub-populations, highlighting the usefulness of surveillance data and/or estimates for both host and vector densities. Elements of Equation (3.1) also show how our applications will rely on an understanding of how mosquito, human and viral traits respond in settings beyond the laboratory, which would involve a combination of laboratory and field/semi-field data.

Equation (3.1) assumes that the infection processes $b_{VE}(t, a_V)$ and $b_{IW}(t, a_I)$ describe density-dependent transmission. Similarly, we can see how elements of the Ross-Macdonald theory and its extensions (Smith et al., 2012, 2014) could be incorporated in our framework, primarily via the processes of Equation (3.1). While the set of Ross-Macdonald models often vary in their structure, we could, for example, embed many core assumptions (Smith et al., 2012) such as a fixed human population count (N^H), latent periods (λ_{Latent}) and biting rates (b), while mosquito mortality could remain age-independent in our framework (as in Equations 2.21–2.32).

Our framework is based on a deterministic model of pathogen dynamics, which models the density of each life stage by continuous variables. Because of this, it is likely most appropriate for modelling the dynamics of larger populations. Particularly for small population counts, it would be useful to develop a stochastic individual-based theory of population dynamics and to explore the relationship between these results and ours, as has previously been considered for directly transmitted diseases (Curran-Sebastian et al., 2025; Pakkanen et al., 2023). These stochastic models may also offer a more natural framework for inferring their parameters (including $R(t)$) than our deterministic model.

The key advance of our research is to derive renewal equations from first principles that can be used to model host-vector disease outbreaks. Since renewal equations form the basis of methods for inferring characteristics of pathogen transmission (e.g. $R(t)$) in real-time during outbreaks, we hope that this research is an initial step towards enabling public health policy advisors to track pathogen transmission more effectively during future outbreaks of a wide range of mosquito-borne diseases (Landau, 2021).

AUTHOR CONTRIBUTIONS

All authors approved the final submitted draft. Cathal Mills and Ben Lambert conceived the idea and methodology for the project. All authors designed and approved the original and final submitted drafts. For the purpose of Open Access, the author has applied a CC BY public copyright licence to any Author Accepted Manuscript version arising from this submission.

ACKNOWLEDGEMENTS

C.M. is supported by a studentship (EP/T517811/1) from the UK's Engineering and Physical Sciences Research Council. T.A. wishes to acknowledge the financial support of the Kuwait Foundation for the Advancement of Sciences (KFAS). K.V.P. acknowledges funding from the MRC Centre for Global Infectious Disease Analysis (Reference No. MR/X020258/1) funded by the UK Medical Research Council. This UK-funded grant is carried out in the frame of the Global Health EDCTP3 Joint Undertaking. M.U.G.K. and C.A.D. acknowledge funding from the Oxford Martin School Programme in Digital Pandemic Preparedness. Grants from the National Secretary of Science FID-2024-146 and FID-2024-147. M.U.G.K. acknowledges funding from The Rockefeller Foundation (PC-2022-POP-005), Google.org, the Oxford Martin School Programme in Pandemic Genomics, European Union's Horizon Europe programme projects MOOD (No. 874850) and E4Warning (No. 101086640), Wellcome Trust grants 303666/Z/23/Z, 226052/Z/22/Z & 228186/Z/23/Z, the United Kingdom Research and Innovation (No. APP8583), the Medical Research Foundation (MRF-RG-ICCH-2022-100069), UK International Development (301542-403), the Bill & Melinda Gates Foundation (INV-063472) and Novo Nordisk Foundation (NNF24OC0094346). C.A.D. is supported by the UK National Institute for Health Research Health Protection Research Unit (NIHR HPRU) in Emerging and Zoonotic Infections in partnership with Public Health England (PHE), Grant Number: HPRU200907. The funders had no role in the study design, analysis or interpretation of results.

CONFLICT OF INTEREST STATEMENT

The authors declare no competing interests.

PEER REVIEW

The peer review history for this article is available at https://www.webofscience.com/api/gateway/wos/peer-review/10.1111/2041-210X.70110.

DATA AVAILABILITY STATEMENT

All code and data used in this article are available at https://doi.org/10.5281/zenodo.15828898 (Mills, 2025).

ORCID

Cathal Mills https://orcid.org/0009-0004-2441-0263
Kris V. Parag https://orcid.org/0000-0002-7806-3605

REFERENCES

Abbott, S., Hellewell, J., Thompson, R. N., Sherratt, K., Gibbs, H. P., Bosse, N. I., Munday, J. D., Meakin, S., Doughty, E. L., Chun, J. Y., Chan, Y.-W. D., Finger, F., Campbell, P., Endo, A., Pearson, C. A. B., Gimma, A., Russell, T., CMMID COVID modelling group, Flasche, S., … Funk, S. (2020). Estimating the time-varying reproduction number of SARS-CoV-2 using national and subnational case counts. *Wellcome Open Research*, *5*, 112. https://doi.org/10.12688/wellcomeopenres.16006.2

Bouros, I., Thompson, R., Gavaghan, D., & Lambert, B. (2025). The time-dependent reproduction number for epidemics in heterogeneous populations. arXiv:2501.17355 [q-bio] http://arxiv.org/abs/2501.17355

Breda, D., Diekmann, O., De Graaf, W. F., Pugliese, A., & Vermiglio, R. (2012). On the formulation of epidemic models (an appraisal of Kermack and McKendrick). *Journal of Biological Dynamics*, *6*, 103–117. https://doi.org/10.1080/17513758.2012.716454

Brouwer, A. F. (2022). Why the Spectral Radius? An intuition-building introduction to the basic reproduction number. *Bulletin of Mathematical Biology*, *84*(9), 96. https://doi.org/10.1007/s11538-022-01057-9

Champredon, D., Dushoff, J., & Earn, D. J. D. (2018). Equivalence of the Erlang-distributed SEIR epidemic model and the renewal equation. *SIAM Journal on Applied Mathematics*, *78*(6), 3258–3278. https://doi.org/10.1137/18M1186411

Chan, M., & Johansson, M. A. (2012). The incubation periods of dengue viruses. *PLoS One*, *7*(11), e50972. https://doi.org/10.1371/journal.pone.0050972

Chen, Y., Xu, Y., Wang, L., Liang, Y., Li, N., Lourenço, J., Yang, Y., Lin, Q., Wang, L., Zhao, H., Cazelles, B., Song, H., Liu, Z., Wang, Z., Brady, O. J., Cauchemez, S., & Tian, H. (2024). Indian Ocean temperature anomalies predict long-term global dengue trends. *Science*, *384*(6696), 639–646. https://doi.org/10.1126/science.adj4427

Codeço, C. T., Villela, D. A., & Coelho, F. C. (2018). Estimating the effective reproduction number of dengue considering temperature-dependent generation intervals. *Epidemics*, *25*, 101–111. https://doi.org/10.1016/j.epidem.2018.05.011

Cori, A., Ferguson, N. M., Fraser, C., & Cauchemez, S. (2013). A new framework and software to estimate time-varying reproduction numbers during epidemics. *American Journal of Epidemiology*, *178*(9), 1505–1512. https://doi.org/10.1093/aje/kwt133

Curran-Sebastian, J., Andersen, F. M., & Bhatt, S. (2025). Modelling the stochastic importation dynamics and establishment of novel pathogenic strains using a general branching processes framework. *Mathematical Biosciences*, *380*, 109352. https://doi.org/10.1016/j.mbs.2024.109352

Dennington, N. L., Grossman, M. K., Teeple, J. L., Johnson, L. R., Shocket, M. S., McGraw, E. A., & Thomas, M. B. (2025). Local adaptation of the mosquito vector, *Aedes aegypti*, and implications for predicting the effects of temperature and climate change on dengue transmission. https://www.biorxiv.org/content/10.1101/2025.02.14.637444v1

Diekmann, O., & Heesterbeek, J. A. P. (2000). Mathematical epidemiology of infectious diseases: model building, analysis and interpretation. In *Wiley series in mathematical and computational biology*. Wiley.

Fraser, C. (2007). Estimating individual and household reproduction numbers in an emerging epidemic. *PLoS One*, *2*(8), e758. https://doi.org/10.1371/journal.pone.0000758

Funk, S., Kucharski, A. J., Camacho, A., Eggo, R. M., Yakob, L., Murray, L. M., & Edmunds, W. J. (2016). Comparative analysis of dengue and Zika outbreaks reveals differences by setting and virus. *PLoS Neglected Tropical Diseases*, *10*(12), e0005173. https://doi.org/10.1371/journal.pntd.0005173

Hersbach, H., Bell, B., Berrisford, P., Hirahara, S., Horányi, A., Muñoz-Sabater, J., Nicolas, J., Peubey, C., Radu, R., Schepers, D., Simmons, A., Soci, C., Abdalla, S., Abellan, X., Balsamo, G., Bechtold, P., Biavati, G., Bidlot, J., Bonavita, M., … Thépaut, J. (2020). The ERA5 global reanalysis. *Quarterly Journal of the Royal Meteorological Society*, *146*(730), 1999–2049. https://doi.org/10.1002/qj.3803

Huber, J. H., Childs, M. L., Caldwell, J. M., & Mordecai, E. A. (2018). Seasonal temperature variation influences climate suitability for dengue, chikungunya, and Zika transmission. *PLoS Neglected Tropical Diseases*, *12*(5), e0006451. https://doi.org/10.1371/journal.pntd.0006451

Inaba, H., & Nishiura, H. (2008). The state-reproduction number for a multistate class age structured epidemic system and its application to the asymptomatic transmission model. *Mathematical Biosciences*, *216*(1), 77–89. https://doi.org/10.1016/j.mbs.2008.08.005

Keeling, M. J., Keeling, M. J., & Rohani, P. (2008). *Modeling infectious diseases in humans and animals*. Princeton University Press.

Kermack, W. O., & McKendrick, A. G. (1927). A contribution to the mathematical theory of epidemics. *Proceedings of the Royal Society of London. Series A: Mathematical and Physical Sciences*, *115*(772), 700–721.

Keyfitz, B., & Keyfitz, N. (1997). The McKendrick partial differential equation and its uses in epidemiology and population study. *Mathematical and Computer Modelling*, *26*(6), 1–9. https://doi.org/10.1016/S0895-7177(97)00165-9

Lambert, B., North, A., & Godfray, H. C. J. (2022). A meta-analysis of longevity estimates of mosquito Vectors of disease. http://biorxiv.org/lookup/doi/10.1101/2022.05.30.494059

Landau, W. M. (2021). The targets R package: a dynamic Make-like function-oriented pipeline toolkit for reproducibility and high-performance computing. *Journal of Open Source Software*, *6*(57), 2959. https://doi.org/10.21105/joss.02959

McKendrick, A. G. (1925). Applications of mathematics to Medical problems. *Proceedings of the Edinburgh Mathematical Society*, *44*, 98–130. https://doi.org/10.1017/S0013091500034428

Meteorological Service Singapore. (2024). Historical daily records. https://www.weather.gov.sg/climate-historical-daily/

Metz, J. A. J., & Diekmann, O. (1986). The dynamics of physiologically structured populations. In *Lecture notes in biomathematics* (Vol. *68*). Springer-Verl.

Mills, C. (2025). cathalmills/vbd_renewal: Pre-publication release, July 2025. https://zenodo.org/doi/10.5281/zenodo.15828897

Monteiro, D. C. S., De Souza, N. V., Amaral, J. C., De Lima, K. B., De Araújo, F. M. C., Ramalho, I. L. C., Martins, V. E. P., Colares, J. K. B., De Góes Cavalcanti, L. P., & Lima, D. M. (2019). Dengue: 30 years of cases in an endemic area. *Clinics*, *74*, e675. https://doi.org/10.6061/clinics/2019/e675

Mordecai, E. A., Caldwell, J. M., Grossman, M. K., Lippi, C. A., Johnson, L. R., Neira, M., Rohr, J. R., Ryan, S. J., Savage, V., Shocket, M. S., Sippy, R., Stewart Ibarra, A. M., Thomas, M. B., & Villena, O. (2019). Thermal biology of mosquito-borne disease. *Ecology Letters*, *22*(10), 1690–1708. https://doi.org/10.1111/ele.13335

Mordecai, E. A., Cohen, J. M., Evans, M. V., Gudapati, P., Johnson, L. R., Lippi, C. A., Miazgowicz, K., Murdock, C. C., Rohr, J. R., Ryan, S. J., Savage, V., Shocket, M. S., Stewart Ibarra, A., Thomas, M. B., & Weikel, D. P. (2017). Detecting the impact of temperature on transmission of Zika, dengue, and chikungunya using mechanistic models. *PLoS Neglected Tropical Diseases*, *11*(4), e0005568. https://doi.org/10.1371/journal.pntd.0005568

Murray, J. D. (2002). *Mathematical biology* (Number 17–18 in Interdisciplinary applied mathematics) (3rd ed.). Springer.

Ogi-Gittins, I., Hart, W., Song, J., Nash, R., Polonsky, J., Cori, A., Hill, E., & Thompson, R. (2023). A simulation-based approach for estimating the time-dependent reproduction number from temporally aggregated disease incidence time series data. http://medrxiv.org/lookup/doi/10.1101/2023.09.13.23295471

Ong, J., Soh, S., Ho, S. H., Seah, A., Dickens, B. S., Tan, K. W., Koo, J. R., Cook, A. R., Richards, D. R., Gaw, L. Y.-F., Ng, L. C., & Lim, J. T. (2022). Fine-scale estimation of effective reproduction numbers for dengue surveillance. *PLoS Computational Biology*, *18*(1), e1009791. https://doi.org/10.1371/journal.pcbi.1009791

Pakkanen, M. S., Miscouridou, X., Penn, M. J., Whittaker, C., Berah, T., Mishra, S., Mellan, T. A., & Bhatt, S. (2023). Unifying incidence and prevalence under a time-varying general branching process. *Journal of Mathematical Biology*, *87*(2), 35. https://doi.org/10.1007/s00285-023-01958-w

Parag, K. V. (2021). Improved estimation of time-varying reproduction numbers at low case incidence and between epidemic waves. *PLoS Computational Biology*, *17*(9), e1009347. https://doi.org/10.1371/journal.pcbi.1009347

Parag, K. V., Cowling, B. J., & Lambert, B. (2023). Angular reproduction numbers improve estimates of transmissibility when disease generation times are misspecified or time-varying. *Proceedings of the Royal Society B: Biological Sciences*, *290*(2007), 20231664. https://doi.org/10.1098/rspb.2023.1664

Parag, K. V., Thompson, R. N., & Donnelly, C. A. (2022). Are epidemic growth rates more informative than reproduction numbers? *Journal of the Royal Statistical Society: Series A (Statistics in Society)*, *185*, S5–S15. https://doi.org/10.1111/rssa.12867

Park, S. W., Akhmetzhanov, A. R., Charniga, K., Cori, A., Davies, N. G., Dushoff, J., Funk, S., Gostic, K., Grenfell, B., Linton, N. M., Lipsitch, M., Lison, A., Overton, C. E., Ward, T., & Abbott, S. (2024). Estimating epidemiological delay distributions for infectious diseases. https://doi.org/10.1101/2024.01.12.24301247

Park, S. W., Bolker, B. M., Funk, S., Metcalf, C. J. E., Weitz, J. S., Grenfell, B. T., & Dushoff, J. (2022). The importance of the generation interval in investigating dynamics and control of new SARS-CoV-2 variants. *Journal of the Royal Society Interface*, *19*(191), 20220173. https://doi.org/10.1098/rsif.2022.0173

Pellis, L., Birrell, P. J., Blake, J., Overton, C. E., Scarabel, F., Stage, H. B., Brooks-Pollock, E., Danon, L., Hall, I., House, T. A., Keeling, M. J., Read, J. M., JUNIPER Consortium, & De Angelis, D. (2022). Estimation of reproduction numbers in real time: Conceptual and statistical challenges. *Journal of the Royal Statistical Society. Series A, Statistics in Society*, *185*(Supplement_1), S112–S130. https://doi.org/10.1111/rssa.12955

Perkins, T. A., Metcalf, C. J. E., Grenfell, B. T., & Tatem, A. J. (2015). Estimating drivers of autochthonous transmission of chikungunya virus in its invasion of the Americas. *PLoS Currents*, *7*, ecurrents.outbreaks.a4c7b6ac10e0420b1788c9767946d1fc. https://doi.org/10.1371/currents.outbreaks.a4c7b6ac10e0420b1788c9767946d1fc

Romeo-Aznar, V., Telle, O., Santos-Vega, M., Paul, R., & Pascual, M. (2024). Crowded and warmer: Unequal dengue risk at high spatial resolution across a megacity of India. *PLOS Climate*, *3*(3), e0000240. https://doi.org/10.1371/journal.pclm.0000240

Ross, R. (1910). *The prevention of malaria*. E.P. Dutton & Company. https://books.google.com/books?id=0jRaWNX-s0C

Scire, J., Huisman, J. S., Grosu, A., Angst, D. C., Lison, A., Li, J., Maathuis, M. H., Bonhoeffer, S., & Stadler, T. (2023). estimateR: an R package to estimate and monitor the effective reproductive number. *BMC Bioinformatics*, *24*(1), 310. https://doi.org/10.1186/s12859-023-05428-4

Shocket, M. S., Verwillow, A. B., Numazu, M. G., Slamani, H., Cohen, J. M., El Moustaid, F., Rohr, J., Johnson, L. R., & Mordecai, E. A. (2020). Transmission of West Nile and five other temperate mosquito-borne viruses peaks at temperatures between 23°C and 26°C. *eLife*, *9*, e58511. https://doi.org/10.7554/eLife.58511

Siraj, A. S., Oidtman, R. J., Huber, J. H., Kraemer, M. U. G., Brady, O. J., Johansson, M. A., & Perkins, T. A. (2017). Temperature modulates dengue virus epidemic growth rates through its effects on reproduction numbers and generation intervals. *PLoS Neglected Tropical Diseases*, *11*(7), e0005797. https://doi.org/10.1371/journal.pntd.0005797

Smith, D. L., Battle, K. E., Hay, S. I., Barker, C. M., Scott, T. W., & McKenzie, F. E. (2012). Ross, Macdonald, and a theory for the dynamics and control of mosquito-transmitted pathogens. *PLoS Pathogens*, *8*(4), e1002588. https://doi.org/10.1371/journal.ppat.1002588

Smith, D. L., Perkins, T. A., Reiner, R. C., Jr., Barker, C. M., Niu, T., Chaves, L. F., Ellis, A. M., George, D. B., Le Menach, A., Pulliam, J. R. C., Bisanzio, D., Buckee, C., Chiyaka, C., Cummings, D. A. T., Garcia, A. J., Gatton, M. L., Gething, P. W., Hartley, D. M., Johnston, G., … Scott, T. W. (2014). Recasting the theory of mosquito-borne pathogen transmission dynamics and control. *Transactions of the Royal Society of Tropical Medicine and Hygiene*, *108*(4), 185–197. https://doi.org/10.1093/trstmh/tru026

Svensson, A. (2007). A note on generation times in epidemic models. *Mathematical Biosciences*, *208*(1), 300–311. https://doi.org/10.1016/j.mbs.2006.10.010

Tesla, B., Demakovsky, L. R., Mordecai, E. A., Ryan, S. J., Bonds, M. H., Ngonghala, C. N., Brindley, M. A., & Murdock, C. C. (2018). Temperature drives Zika virus transmission: evidence from empirical and mathematical models. *Proceedings of the Royal Society B: Biological Sciences*, *285*(1884), 20180795. https://doi.org/10.1098/rspb.2018.0795

Thompson, R., Stockwin, J., Van Gaalen, R., Polonsky, J., Kamvar, Z., Demarsh, P., Dahlqwist, E., Li, S., Miguel, E., Jombart, T., Lessler, J., Cauchemez, S., & Cori, A. (2019). Improved inference of time-varying reproduction numbers during infectious disease outbreaks. *Epidemics*, *29*, 100356. https://doi.org/10.1016/j.epidem.2019.100356

Vegvari, C., Abbott, S., Ball, F., Brooks-Pollock, E., Challen, R., Collyer, B. S., Dangerfield, C., Gog, J. R., Gostic, K. M., Heffernan, J. M., Hollingsworth, T. D., Isham, V., Kenah, E., Mollison, D., Panovska-Griffiths, J., Pellis, L., Roberts, M. G., Scalia Tomba, G., Thompson, R. N., & Trapman, P. (2022). Commentary on the use of the reproduction number *R* during the COVID-19 pandemic. *Statistical Methods in Medical Research*, *31*(9), 1675–1685. https://doi.org/10.1177/09622802211037079

Wallinga, J., & Lipsitch, M. (2007). How generation intervals shape the relationship between growth rates and reproductive numbers. *Proceedings of the Royal Society B: Biological Sciences*, *274*(1609), 599–604. https://doi.org/10.1098/rspb.2006.3754

Yang, H. M., Macoris, M. L. G., Galvani, K. C., Andrighetti, M. T. M., & Wanderley, D. M. V. (2009). Assessing the effects of temperature on the population of *Aedes aegypti*, the vector of dengue. *Epidemiology and Infection*, *137*(8), 1188–1202. https://doi.org/10.1017/S0950268809002040

SUPPORTING INFORMATION

Additional supporting information can be found online in the Supporting Information section at the end of this article.

Appendix A. Renewal equations, generation times, and McKendrick–von Foer ster equations.

Appendix B. Exposure-and-infection-age-structured human and infection-age structured mosquito population.

Appendix C. Exposure-and-infection-age-structured human and infection-age structured mosquito population.

Appendix D. Exposure-and-infection-age-structured populations of human and mosquitoes.

Figure S1. Time-varying generation times in Ang Mo Kio, Singapore.

Figure S2. Time-varying generation times in Ang Mo Kio, Singapore.

Figure S3. Time-varying generation times in São João do Tauape, Fortaleza, Brazil.

Figure S4. Time-varying generation times in São João do Tauape, Fortaleza, Brazil.

Figure S5. Time-varying generation times in our simulated environment.

Figure S6. Time-varying generation times in our simulated environment.

How to cite this article: Mills, C., Alrefae, T., Hart, W. S., Kraemer, M. U. G., Parag, K. V., Thompson, R. N., Donnelly, C. A., & Lambert, B. (2025). Renewal equations for mosquito-borne diseases. *Methods in Ecology and Evolution*, *16*, 2653–2666. https://doi.org/10.1111/2041-210X.70110